

Supporting Information

Ni-N synergy enhanced synthesis of formic acid via CO₂ hydrogenation under mild condition

Jyotishman Kaishyop^{a,b}, Tuhin Suvra Khan^{a,b}, Satyajit Panda^{a,b}, Chandewar Pranay Rajendra^c, Debaprashad Shee^c, Tulio C. R. Rocha^d, Flavio C. Vicentin^d, Ankur Bordoloi^{a,b,*}

[a] Light Stock Processing Division

CSIR-Indian Institute of Petroleum

Mohkampur, Haridwar road, Dehradun, Uttarakhand – 248005

[b] Academy of Scientific and Innovative Research (AcSIR)

Ghaziabad- 201002, India

[c] Department of Chemical Engineering

Indian Institute of Technology Hyderabad

Kandi, Telangana – 502284

[d] Brazilian Synchrotron Light Laboratory (LNLS),

Brazilian Center for Research on Energy and Materials (CNPEM), 13083-100, Brazil

Table of Contents

Table S1	The amount of CO ₂ desorbed in the CO ₂ -TPD experiment	3
Table S2	Catalytic recyclability of 1Ni/N-TiO ₂	3
Table S3	The representation of deviation in CO ₂ hydrogenation for 1Ni/N-TiO ₂ catalyst	3
Figure S1	Raman spectrum	4
Figure S2	H ₂ TPR profile.....	5
	CO ₂ adsorption isotherm	6
Figure S3	CO ₂ adsorption isotherm at 1 bar and 298 K	6
Figure S4	DFT optimised structure of (a) Ni ₁₃ /2N-TiO ₂ (101) surface (b) Ni ₁₃ /4N-TiO ₂ (101) surface, and (c) Ni ₁₃ /6N-TiO ₂ (101) surface	7
	Effect of nitrogen content on CO ₂ adsorption	7
Figure S5	DFT optimised geometry of the CO ₂ adsorption at (a) Ni ₁₃ /2N-TiO ₂ (101) surface (b) Ni ₁₃ /4N-TiO ₂ (101) surface, and (c) Ni ₁₃ /6N-TiO ₂ (101) surface	8

Table S1: The amount of CO₂ desorbed in the CO₂-TPD experiments.

Sl. No.	Catalysts	CO ₂ Desorbed (cm ³ /g STP)				CO ₂ uptake capacity (mmol/g)	Conversion (%)
		Weak	Intermediate	High	Total		
1	2.5Ni/N-TiO ₂	0.1367	0.0834	-	0.2201	0.3	9.6
2	1.0Ni/N-TiO ₂	0.0927	0.1384	-	0.2311	0.39	11.29
3	0.5Ni/N-TiO ₂	0.1535	0.0587	-	0.2122	0.24	7.79
4	1.0Ni/TiO ₂	0.2062	0	-	0.2062	0.23	7.39

Table S2: Catalytic recyclability of 1Ni/N-TiO₂ catalyst

Cycle	Conversion (%)	TON
Cycle 1	11.29	757
Cycle 2	11.28	755
Cycle 3	11.26	752
Cycle 4	11.25	749

Reaction condition: Catalyst amount: 100 mg, Solvent: H₂O, Temperature: 353 K, Pressure: 60 bar, Time: 20 h

Table S3: The representation of deviation in CO₂ hydrogenation for 1Ni/N-TiO₂ catalyst

Batch	Conversion (%)	TON
Batch 1	11.29	757
Batch 2	11.28	755
Batch 3	11.17	750
Batch 4	11.27	754
Average	11.25	754
Standard deviation	0.06	2.94

Reaction condition: Catalyst amount: 100 mg, Solvent: H₂O, Temperature: 353 K, Pressure: 60 bar, Time: 20 h

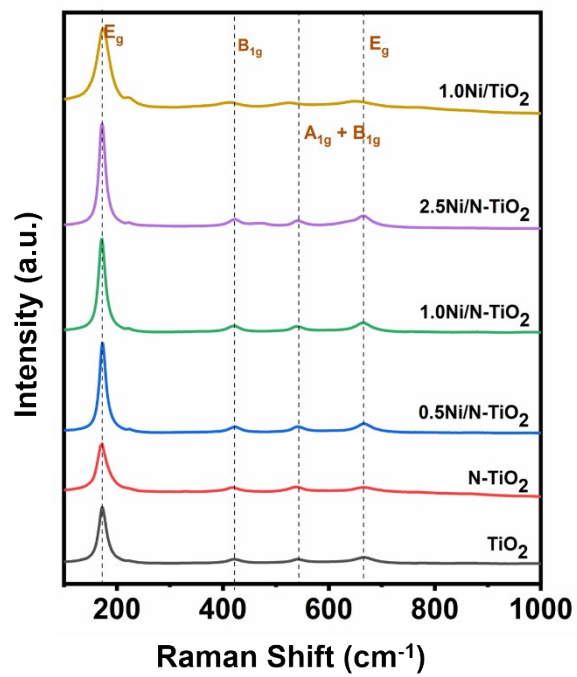


Figure S1: Raman Spectrum

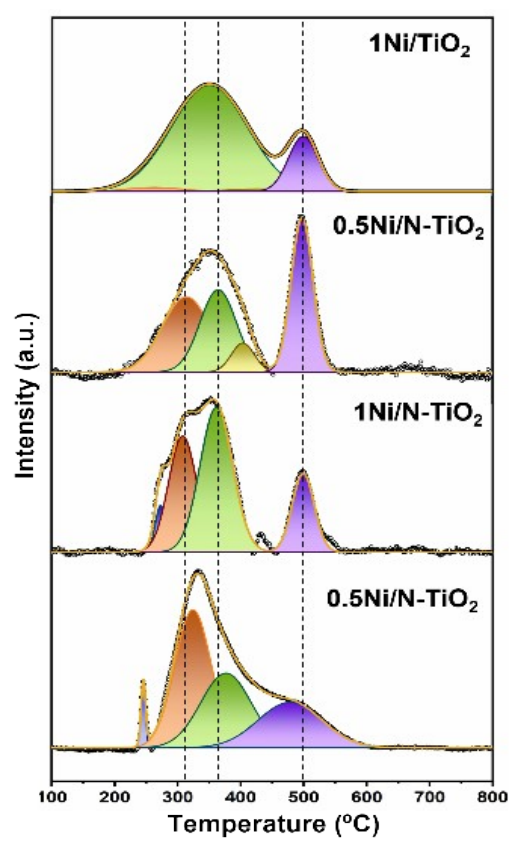


Figure S2: H₂-TPR profile

CO₂ adsorption isotherm

The CO₂ adsorption performance of as-prepared catalysts, including 2.5Ni/N-TiO₂, 1Ni/N-TiO₂, 0.5Ni/N-TiO₂, and 1Ni/TiO₂, were studied at 1 bar pressure and 298 K temperature, as shown in Fig. S3. Remarkably, the 1Ni/N-TiO₂ catalyst showed highest adsorption capacity of 0.39 mmol per g of catalyst, followed by 2.5 Ni/N-TiO₂ catalyst with adsorption capacity of 0.3 mmol/g. The lower adsorption capacity of 2.5 Ni/N-TiO₂ compared to 1Ni/N-TiO₂ is due to a lower surface area caused by higher metal loading. The 0.5 Ni/N-TiO₂ catalyst exhibits an adsorption capacity of 0.24 mmol/g, whereas the N-undoped 1Ni/TiO₂ possesses an adsorption capacity of 0.23 mmol/g at standard temperature and pressure. It has been observed that CO₂ adsorbs strongly on 1Ni/N-TiO₂ as compared to 1Ni/TiO₂. These findings are in accordance with the DFT-predicted CO₂ adsorption behaviour as CO₂ adsorbs on Ni₁₃/N-TiO₂ (101) surface with a binding energy of -0.73 eV; whereas the binding energy of CO₂ on Ni₁₃/TiO₂ was calculated to be -0.50 eV.

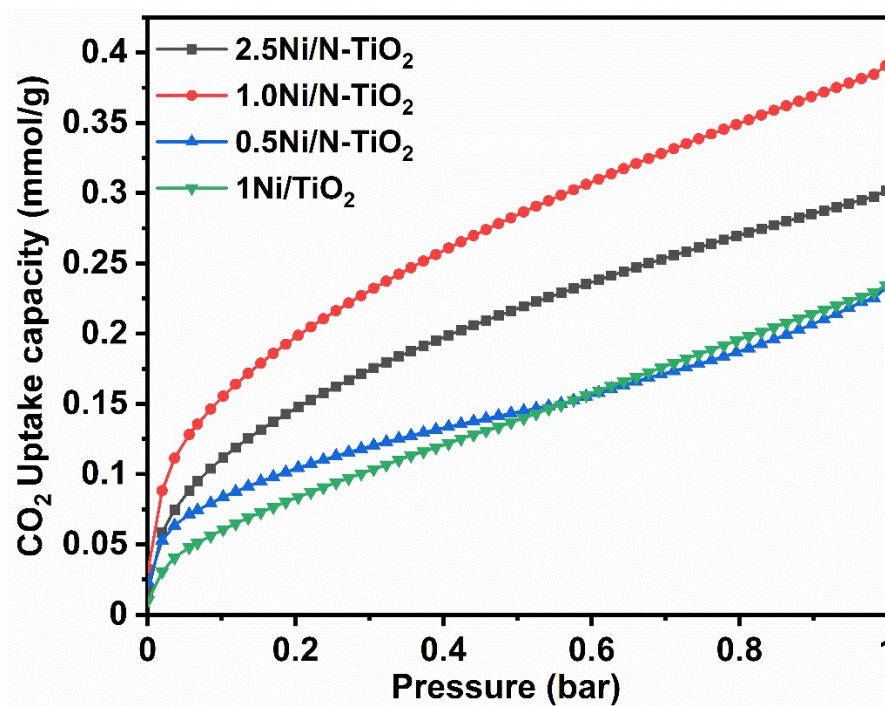


Figure S3: CO₂ adsorption isotherm at 1 bar and 298 K

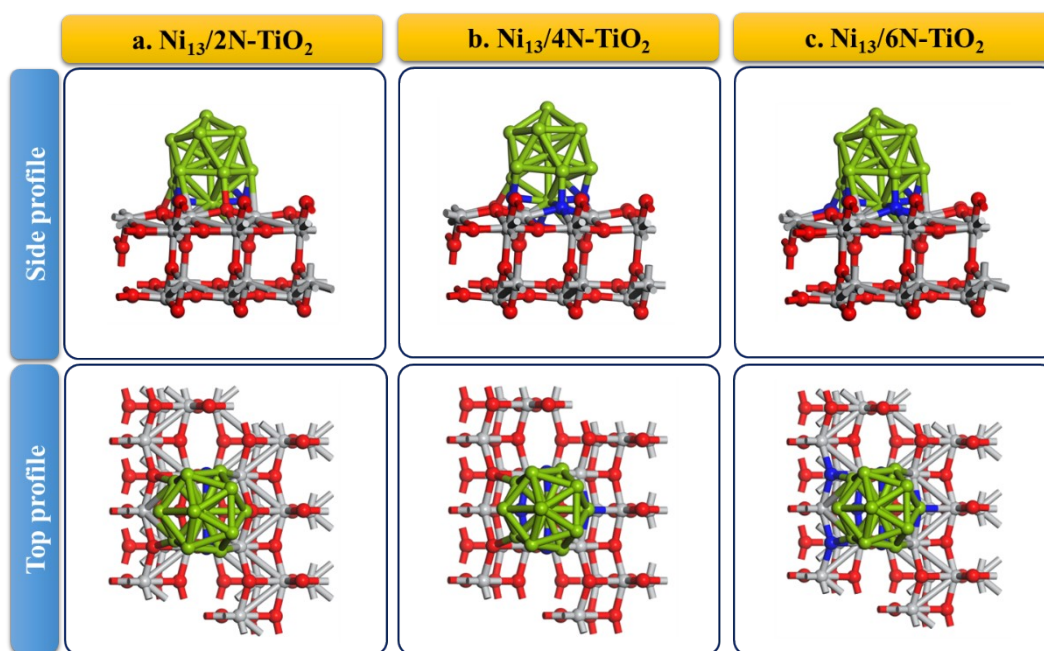


Figure S4: The DFT optimised structure of (a) Ni₁₃/2N-TiO₂ (101) surface (b) Ni₁₃/4N-TiO₂ (101) surface, and (c) Ni₁₃/6N-TiO₂ (101) surface Color code: Green: Nickel, Blue: Nitrogen, Gray: Titanium, and Red: Oxygen

Effect of Nitrogen content on CO₂ adsorption

The adsorption characteristics of CO₂ species on the Ni₁₃/2N-TiO₂ (101) surface and Ni₁₃/6N-TiO₂ (101) surface were investigated, employing the same calculation parameters set for the other calculations in the manuscript. Fig. S5 (a) shows that CO₂ was adsorbed on the Ni₁₃/2N-TiO₂ (101) surface in a bend configuration by forming three bonds, one of which the 'O' atom of CO₂ bonded to a Ni atom with a bond length of 2.09 Å and the rest of 'C' and 'O' atoms were together bonded to a neighbouring Ni atom possessing a bond length of 1.89 Å and 2.19 Å, respectively. The binding energy calculated for CO₂ on Ni₁₃/2N-TiO₂ was -0.55 eV, slightly higher exothermic than Ni₁₃/TiO₂ by 0.05 eV, which possesses binding energy of -0.50 eV. However, the stability of CO₂ on the Ni₁₃/2N-TiO₂(101) surface was very close to the Ni₁₃/TiO₂ as compared to Ni₁₃/4N-TiO₂, which exhibits a binding energy of -0.73 eV. CO₂ was observed to be adsorbed on Ni₁₃/6N-TiO₂ (101) surface through the formation of three bonds in a similar manner in the case of Ni₁₃/2N-TiO₂, as can be seen in Fig. S5 (c). The bond length of the O-Ni bond was measured to be 2.06 Å, whereas the C-Ni bond and O-Ni bonds were calculated to be 1.88 Å and 2.23 Å, respectively. The binding energy of CO₂ on the Ni₁₃/6N-TiO₂ was computed to be -0.81 eV. It was observed that the binding energy of CO₂ was increased with the increase in the number of N atoms following the trend: Ni₁₃/TiO₂ (-0.5 eV) < Ni₁₃/2N-TiO₂ (-0.55 eV) < Ni₁₃/4N-TiO₂ (-0.73 eV) < Ni₁₃/6N-TiO₂ (-0.81 eV). This study reveals that the increasing number of N atoms enhances the basicity of the catalyst surface, due to which the acid-base interaction between the basic catalyst surface and the acidic CO₂ has increased, resulting in the stable adsorption of CO₂. However, if compared to Ni₁₃/TiO₂

surface, the adsorption of the CO₂ species was slightly exothermic by 0.05 eV on Ni₁₃/2N-TiO₂ surface, whereas it was significantly more exothermic on the Ni₁₃/4N-TiO₂ surface by 0.23 eV. Further increasing the number of N atoms on the Ni₁₃/4N-TiO₂ surface makes the CO₂ adsorption process higher exothermic. Nevertheless, the CO₂ adsorbs on Ni₁₃/6N-TiO₂ surface with a small increment of binding energy than Ni₁₃/4N-TiO₂ surface by 0.08 eV, relatively very close to Ni₁₃/4N-TiO₂ surface.

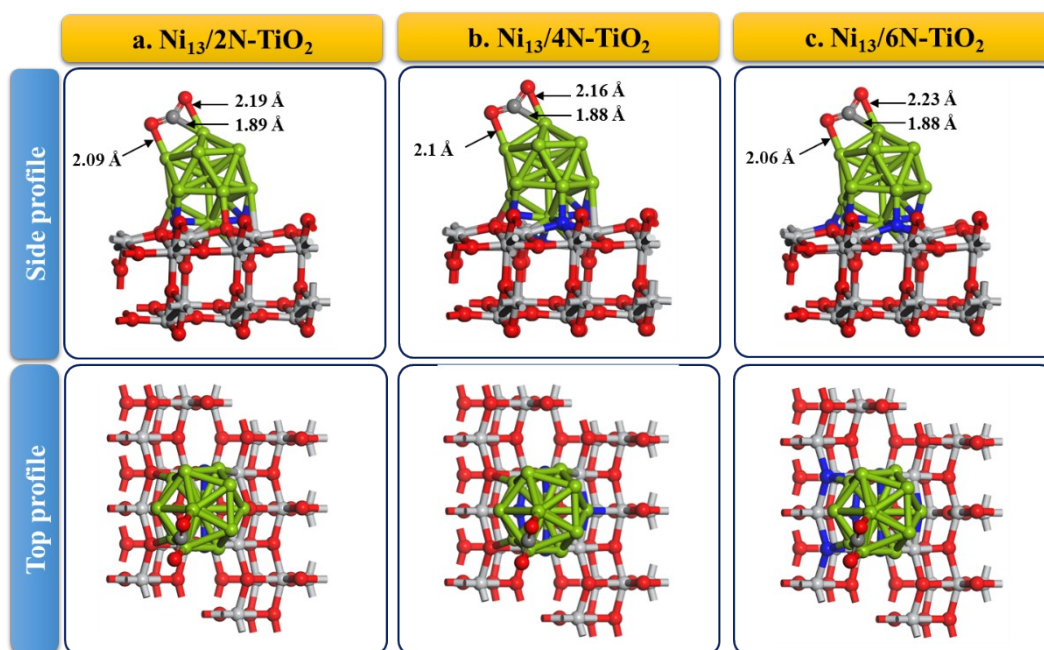


Figure S5: The DFT optimised geometry of the CO₂ adsorption at (a) Ni₁₃/2N-TiO₂ (101) surface (b) Ni₁₃/4N-TiO₂ (101) surface, and (c) Ni₁₃/6N-TiO₂ (101) surface Color code: Green: Nickel, Blue: Nitrogen, Gray: Titanium, Dark Gray: Carbon and Red: Oxygen

The stable configuration of the Ni₁₃/6N-TiO₂ model possesses no Ni-O bonding, as shown in Fig. 1 (c), which is not supported by catalyst characterization evidence, as discussed earlier. In contrast, Ni₁₃/4N-TiO₂ exhibited a significant enhancement in CO₂ bind energy than Ni₁₃/TiO₂, along with supporting the characterization data. Therefore, Ni₁₃/4N-TiO₂ was chosen to represent 1Ni/N-TiO₂ catalyst for further DFT calculations.